Tribology Letters, Vol. 23, No. 2, August 2006 (© 2006)
DOI: 10.1007/s11249-006-9057-0

Multi-environmental lubrication performance and lubrication mechanism of $MoS_2/Sb_2O_3/C$ composite films

J.S. Zabinski, J.E. Bultman, J.H. Sanders and J.J. Hu*

Materials and Manufacturing Directorate, Air Force Research Laboratory (AFRL/ML), Wright-Patterson Air Force Base, Bldg. 654, 2941 Hobson Way, Dayton, OH 45433-7750, USA

Received 20 January 2006; accepted 20 March 2006; published online 29 August 2006

MoS_2–Sb_2O_3–C composite films exhibit adaptive behavior, where surface chemistry changes with environment to maintain the good friction and wear characteristics. In previous work on nanocomposite coatings grown by PVD, this type of material was called a "chameleon" coating. Coatings used in this report were applied by burnishing mixed powders of MoS_2, Sb_2O_3 and graphite. The solid lubricant MoS_2 and graphite were selected to lubricate over a wide and complementary range including vacuum, dry air and humid air. Sb_2O_3 was used as a dopant because it acts synergistically with MoS_2, improving friction and wear properties. The MoS_2–Sb_2O_3–C composite films showed lower friction and longer wear life than either single component MoS_2 or C film in humid air. Very or even super low friction and long wear-life were observed in dry nitrogen and vacuum. The excellent tribological performance was verified and repeated in cycles between humid air and dry nitrogen. The formation of tribo-films at rubbing contacts was studied to identify the lubricating chemistry and microstructure, which varied with environmental conditions. Micro-Raman spectroscopy and Auger electron spectroscopy (AES) were used to determine surface chemistry, while scanning electron microscopy and transmission electron microscopy were used for microstructural analysis. The tribological improvement and lubrication mechanism of MoS_2–Sb_2O_3–C composite films were caused by enrichment of the active lubricant at the contact surface, alignment of the crystal orientation of the lubricant grains, and enrichment of the non lubricant materials below the surface. Sb_2O_3, which is not lubricious, was covered by the active lubricants (MoS_2 – dry, C – humid air). Clearly, the dynamics of friction during environmental cycling cleaned some Sb_2O_3 particles of one lubricant and coated it with the active lubricant for the specific environment. Mechanisms of lubrication and the role of the different materials will be discussed.

KEY WORDS: molybdenum disulfide, antimony trioxide, graphite, burnish, composite film, multi-environment, lubrication, tribology

1. Introduction

The lubrication performance of MoS_2 has been greatly improved through the use of dopants including inorganic sulfides/oxides [1–9] and metals [10–15]. The dopants that work well are not typically solid lubricants themselves. Yet, they lower friction, increase endurance, enhance load-carrying capacity, and broaden the environmental operating range of lubricant systems. Additional improvements can be realized by mixing two or more types of solid lubricants with an additive. The composite can provide excellent lubrication in multiple environments where low friction is sustained by the active lubricant moving to the interface. For example, MoS_2 and graphite materials are common solid lubricants in dry and humid environments, respectively. Therefore, MoS_2 and graphite composites have the potential to lubricate in both dry and humid environments. One modern technique to make composite lubricants is magnetron assisted pulsed laser deposition, for example, it can produce nanocomposite tribological coatings with "chameleon" surface adaptation [16]. The deposition systems include UHV chambers, pulsed lasers and magnetron sputtering sources, which add cost to the coatings. However, these techniques provide significant advantages such as good adhesion, precise control of thickness, and improved hardness and toughness in addition to lubrication.

For many tribological applications, a simpler deposition may be more cost effective. Composite coatings were deposited by simple burnishing to determine the fundamental mechanism of lubrication and to compare mechanisms with composite coatings grown by PVD. In this study, MoS_2 was used to provide lubrication in dry environments, graphite was used for humid air, and Sb_2O_3 was the dopant. Sb_2O_3 compound was selected because it acts synergistically with MoS_2 so as to improve friction and wear properties [5,6,9]. Compression, shear and crystallite re-orientation occur in the burnished films during running-in [17]. The MoS_2–Sb_2O_3–C composite films showed lower friction and longer wear life than MoS_2 films in humid air. Very/super low friction and long wear-life were measured in dry nitrogen and vacuum. The excellent tribological

*To whom correspondence should be addressed.
E-mail: Jianjun.Hu@WPAFB.AF.MIL

1023-8883/06/0800–0155/0 © 2006 Springer Science+Business Media, Inc.

performance in different environments was verified and repeated in climate cycling between humid air and dry nitrogen. The formation of tribo-films at rubbing contacts was studied in terms of film chemistry and microstructure. Micro Raman spectroscopy and Auger electron spectroscopy (AES) were used to measure changes in surface chemistry, while scanning electron microscopy (SEM) and transmission electron microscopy (TEM) were used for microstructural analysis. The tribological properties and lubrication mechanism of MoS_2–Sb_2O_3–C composite films are understood in terms of the dynamics of lubricant and additive behavior.

2. Experimental

MoS_2–Sb_2O_3–C composite films were burnished on polished 440C stainless steel disks of 25.4 mm diameter by using a lint free cloth under hand pressure. Before deposition, the steel disks were cleaned using soap + water, acetone, and methanol. Pure MoS_2, graphite and Sb_2O_3 powders were mixed together at a ratio of 40:40:20 wt.%. A smooth sliding pressure was applied to the mixed powder against the hard surface of steel substrates. The burnishing process was done in air at approximately 40% relative humidity (RH).

Friction coefficients of burnished MoS_2–Sb_2O_3–C composite films were collected using a ball-on-disc tribometer run with the specimens in the horizontal position at room temperature. The measurements were made in humid air at 50% RH, dry nitrogen at one atmosphere, and high vacuum at 10^{-8} Torr, respectively. Grade 5 440C-stainless steel bearing balls of 6.35 mm diameter were used as the counterface. For each friction trace, a normal load of 100 g was set and the rotational speed was maintained at 200 rpm. The approximate sliding speed was about 100–200 mm s^{-1} depending on wear track radii. After determining that speed within this range did not affect results, no effort was made to maintain constant linear speed. In our present study, failure is defined as an increase in average friction over 0.65. Average friction is calculated using the last 10 data points. Friction measurements in multiple cycles of humid air and dry nitrogen were also collected for evaluating the environmental adaptability of the burnished films. Wear scars were analyzed after the tribotests were stopped with the last environment being humid and dry, respectively, in order to determine the nature of the active lubricating film on the surface.

A Leica 360 field-emission-gun (FEG) SEM, equipped with a Link ISIS X-ray energy dispersive spectrometer (EDS), was used for microstructural observations of wear scars. It was operated at an accelerating voltage of 25 keV and a working distance of 15 mm. Raman spectra were obtained using a Renishaw Ramanscope 2000 equipped with a 514.5 nm argon-ion laser and an air-cooled charge-coupled device (CCD). Raman analysis was used to determine the chemical changes inside wear scars. AES measurements were made using a Physical Electronics PHI 5700 multi-technique system. The electron gun on this system has a minimum electron probe size of 100 nm at 10 keV. AES data were acquired with a concentric hemispherical analyzer at a 45° takeoff angle. A secondary electron detector was used for imaging the wear scar surface and positioning the probe beam. The basic vacuum pressure in the analysis chamber was better than 10^{-7} Pa.

To visualize the film microstructure at the surface of wear scars after the samples were tribotested, lift-out specimens for cross-sectional TEM (XTEM) observations were prepared using a focused ion beam (FIB) microscope, FEI-DB235. It was operated using 5 keV electron beams and 30 keV Ga^+ ion beams. To protect the wear scar surface, an approximate 2 μm thick Pt cap was deposited on the top of wear scars by using a gas injection system. Overall, the process started with electron beam deposition of Pt, which was followed by ion beam deposition at a moderate probe current. High-resolution microstructures of wear scar sections were observed using a Philips CM200-FEG TEM operated at 200 keV. The FEG provided a complete coherent electron source and nm-sized electron probe, which was adjustable from 25 to 1 nm. A NORAN X-ray EDS system attached to the TEM was used for measuring chemical compositions.

3. Results and discussion

3.1. Friction coefficients in humid, dry and vacuum conditions

Tribological data from a ball-on-disk machine are shown in figure 1. It is well known that graphite and hexagonal MoS_2 perform best in humid air and dry nitrogen, respectively. Their tribological properties degrade significantly if the environments are switched. Figure 1a shows the friction traces measured for the burnished graphite film in dry nitrogen, and for the MoS_2 and MoS_2–Sb_2O_3–C composite films in humid air at 50% RH, respectively, so as to compare tribological properties in the harshest environment for each lubricant or lubricant mixture. The burnished MoS_2 film exhibited an erratic friction coefficient of approximately 0.2 and failed after 10,000 cycles. The pure graphite film provided a very low friction coefficient between 0.01 and 0.02 for the first 10,000 cycles, and after that, the friction increased significantly and became erratic. It finally failed after approximately 25,000 cycles. The burnished MoS_2–Sb_2O_3–C composite film showed a steady-state friction coefficient between 0.1 and 0.2 in humid air at 50% RH, and its wear life was approximately 50,000 cycles, as shown in figure 1a. Therefore, the composite film showed a more stable friction coefficient and longer wear life in the harshest environment than the pure

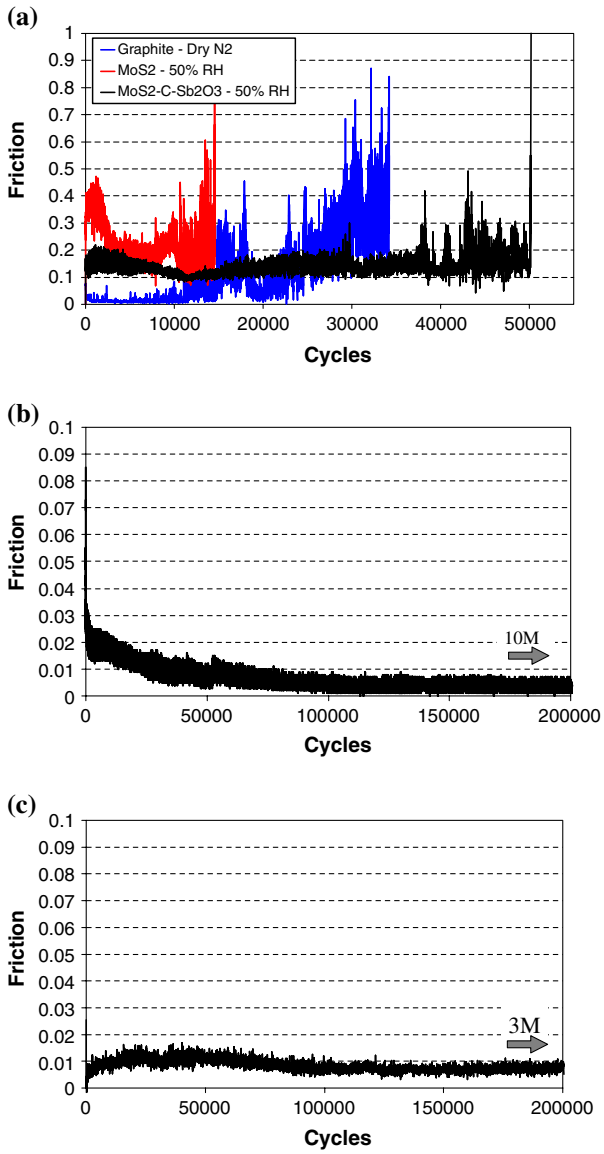

Figure 1. Friction traces from ball-on-disc tribotests of burnished films on steel substrates: (a) in worst environments – graphite in dry nitrogen, MoS_2 in air at 50% relative humidity (RH), and MoS_2–Sb_2O_3–C in air at 50% RH, (b) MoS_2–Sb_2O_3–C in dry nitrogen (The test stopped at 10 million cycles and did not fail), and (c) MoS_2–Sb_2O_3–C in high vacuum at 10^{-8} Torr (The test stopped after 3 million cycles and did not fail).

graphite and hexagonal MoS_2 films. One reason could be that the Sb_2O_3 additives acted synergistically with MoS_2/C so as to improve friction and wear properties [5,6,16]. Another reason could be due to the synergistic effect as observed for graphite/MoS_2 mixtures [18,19].

A super low friction coefficient was measured at as less than 0.01 for the composite film in dry nitrogen and high vacuum (see figure 1b, c), where the tribotests run smoothly and do not show any evidence of failure. The dry nitrogen test was terminated at 10,000,000 cycles without failure, and the high vacuum test was terminated at 3,000,000 cycles without failure. Friction below 0.01 is quite low and strain gauges may drift over time, especially over days like in the dry environment tests. To ensure that the measured friction was really below 0.01, additional tests were run. First, the load was increased to 500 kg to put the friction force more solidly within the capability of the load cell. In addition, the load cell was calibrated before and after each testing. Using the steps outlined, it is concluded that the friction coefficient was ≤ 0.008. Anything below that is outside the confidence level of our equipment. Clearly, the MoS_2–Sb_2O_3–C composite films improved tribological properties compared to the pure, single component films (MoS_2 or C) in a wide range of environments.

3.2. Characterization of worn surfaces

To understand the tribological behavior of burnished MoS_2–Sb_2O_3–C composite films in various environments, a series of analysis techniques was employed to characterize the worn film. Figure 2 shows the Raman spectra collected from the as-burnished MoS_2–Sb_2O_3–C composite film and from the wear scars in humid air, dry nitrogen, and high vacuum, respectively. The features of both hexagonal MoS_2 and graphite are exhibited in the Raman spectra of the wear scars in dry nitrogen and

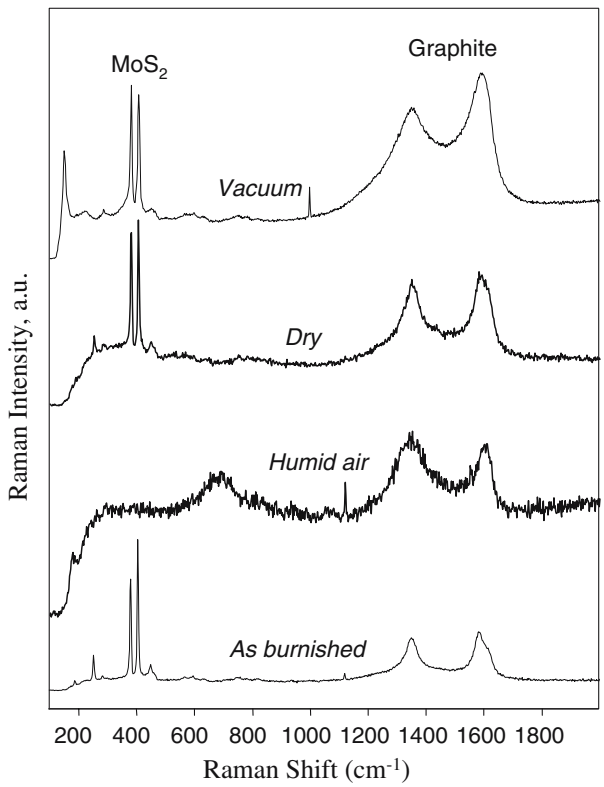

Figure 2. Raman spectra collected from the as-burnished MoS_2–Sb_2O_3–C composite film, and for wear scars in humid air, dry nitrogen and high vacuum, respectively. Typical Raman features of both MoS_2 and graphite are indicated in the spectra from the as-burnished film and wear scars in dry nitrogen and high vacuum, while only graphite feature shows for the wear scar in humid air.

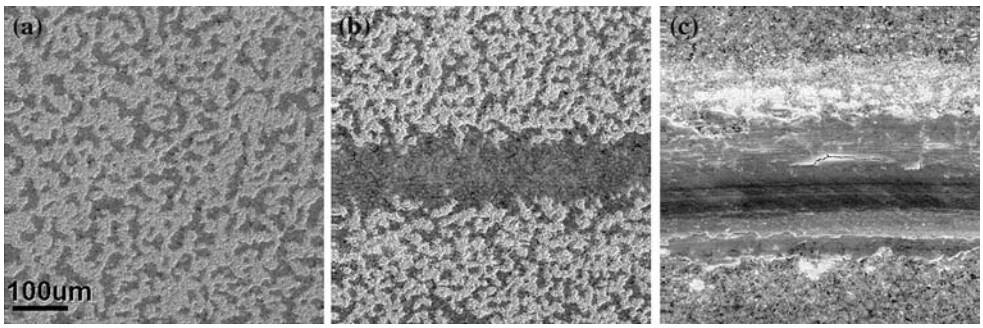

Figure 3. SEM images taken from: (a) the as-burnished MoS_2–Sb_2O_3–C composite film, (b) the wear scar in dry nitrogen, and (c) the wear scar in air at 50% relative humidity (RH).

high vacuum. They look similar to the as-burnished composite film. Only graphite-like features are exhibited in the Raman spectrum of humid air tests. The difference between the Raman spectra of wear scars produced in dry and humid environments suggests that graphite occupied the interface and is the active lubricant in humid air. Hexagonal MoS_2 was present at the interface in dry/vacuum conditions. This finding is in good agreement with measurements of friction coefficients: 0.1–0.2 in humid (typical graphite reading) and around 0.01 in dry/vacuum (typical MoS_2 reading). Although, it is noted that MoS_2 also exhibits friction coefficients in the 0.2 range in humid air.

Figure 3a shows the SEM image of as-burnished MoS_2–Sb_2O_3–C composite films on steel substrates. Figure 3b, c show the SEM images of the wear scars from dry nitrogen (after 100,000 cycles) and humid air at 50% RH (after 10,000 cycles) tests, respectively. They are taken at the same magnification. The MoS_2–Sb_2O_3–C composite film was smeared by rubbing and formed a dense uniform wear track in the dry nitrogen test, as shown in figure 3b. The wear scar was extremely light and virtually no wear had occurred in the "dry" wear track. However, wear in the "humid" wear track was clearly shown in figure 3c, which was accompanied with debris along the side of the track. Cracking was

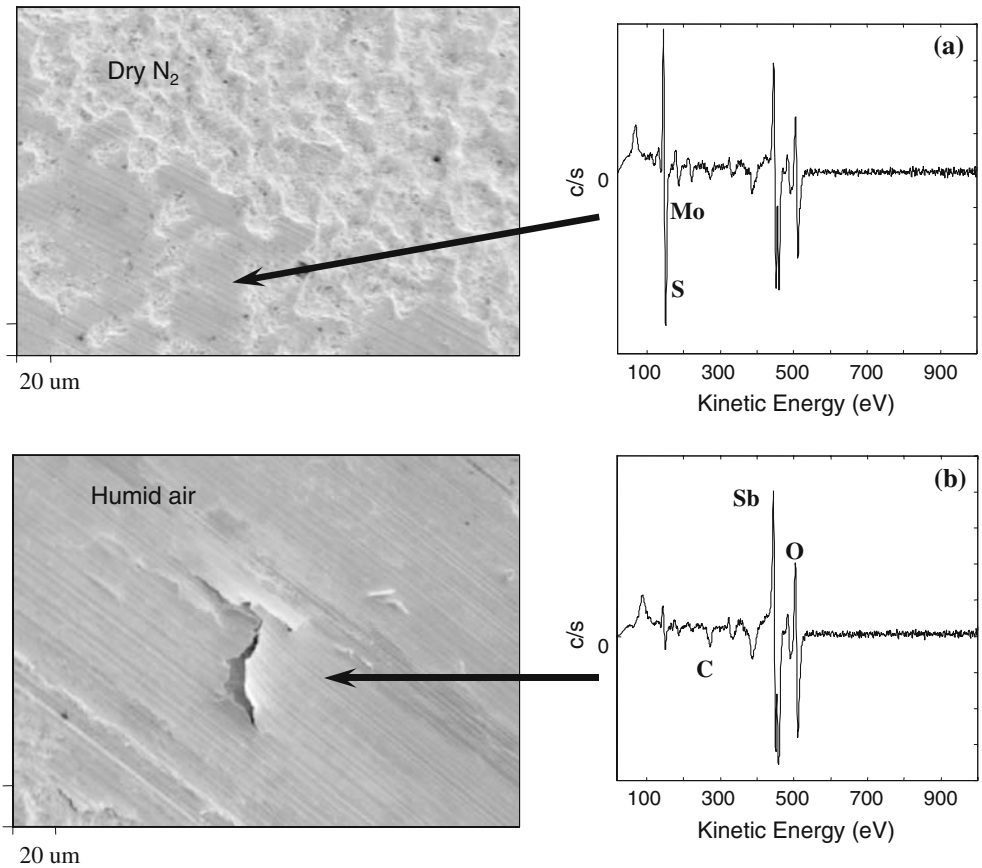

Figure 4. Auger electron spectroscopy (AES) spectra collected from inside the wear scars: (a) in dry nitrogen, and (b) in humid air. The measurement positions are indicated in the corresponding SEM images of wear scars as shown on left.

observed inside the "humid" wear track, as shown in figure 3c. In every wear track created in a moist environment, cracking was observed. In fact, cracking proceeds to failure such that its appearance and severity accompany failure. In long lived film, cracking is inhibited and appears much later in the life cycle.

The surface chemistries of the dry and humid wear scars were further studied by AES, as shown in figure 4a, b. The corresponding SEM images are shown on the left and indicate the exact location of the AES probe on the wear scars. The signal intensity shows a significant amount of MoS_2 inside the dry wear scar, and the signal is greatly diminished inside the humid wear scar. A greater C signal was collected from inside the humid wear scar compared to dry. The AES data complements and agrees with the Raman data. Interestingly, the AES data shows that Sb_2O_3 is in both scars created in humid and dry environments. Sb_2O_3 is generally not observed by Raman on surfaces that have been rubbed. The data suggested that Sb_2O_3 is: (1) below the surface and not detected by Raman but within the escape depth of auger electrons, or (2) altered by rubbing in the near surface region such that it is not detectable by Raman spectroscopy. It is noted that Sb has a very high Auger sensitivity, which may partially explain why its intensity is high. The following cross-sectional TEM analyses provided additional insight.

3.3. FIB/TEM analyses of wear scar cross-sections

A FIB microscope was used to prepare the cross-sectional TEM specimen showing the inside of wear scars for direct observation of film microstructures. Figure 5 shows an electron-transparent foil of about

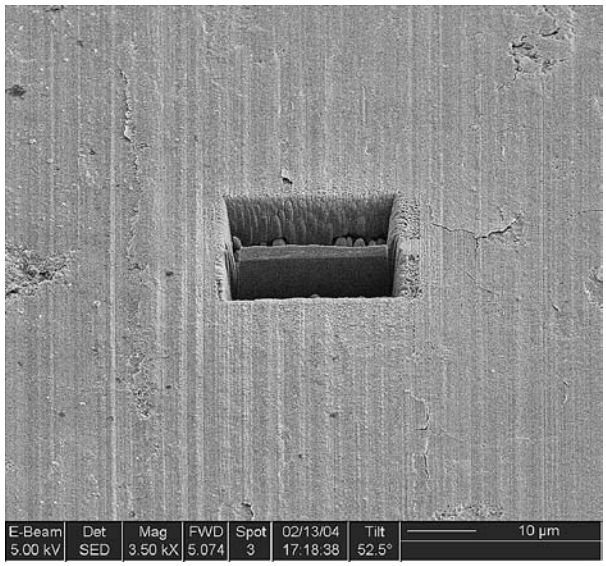

Figure 5. A focused ion beam (FIB) prepared lift-out specimen for the cross-sectional TEM observation of wears scars on the burnished MoS_2–Sb_2O_3–C composite film.

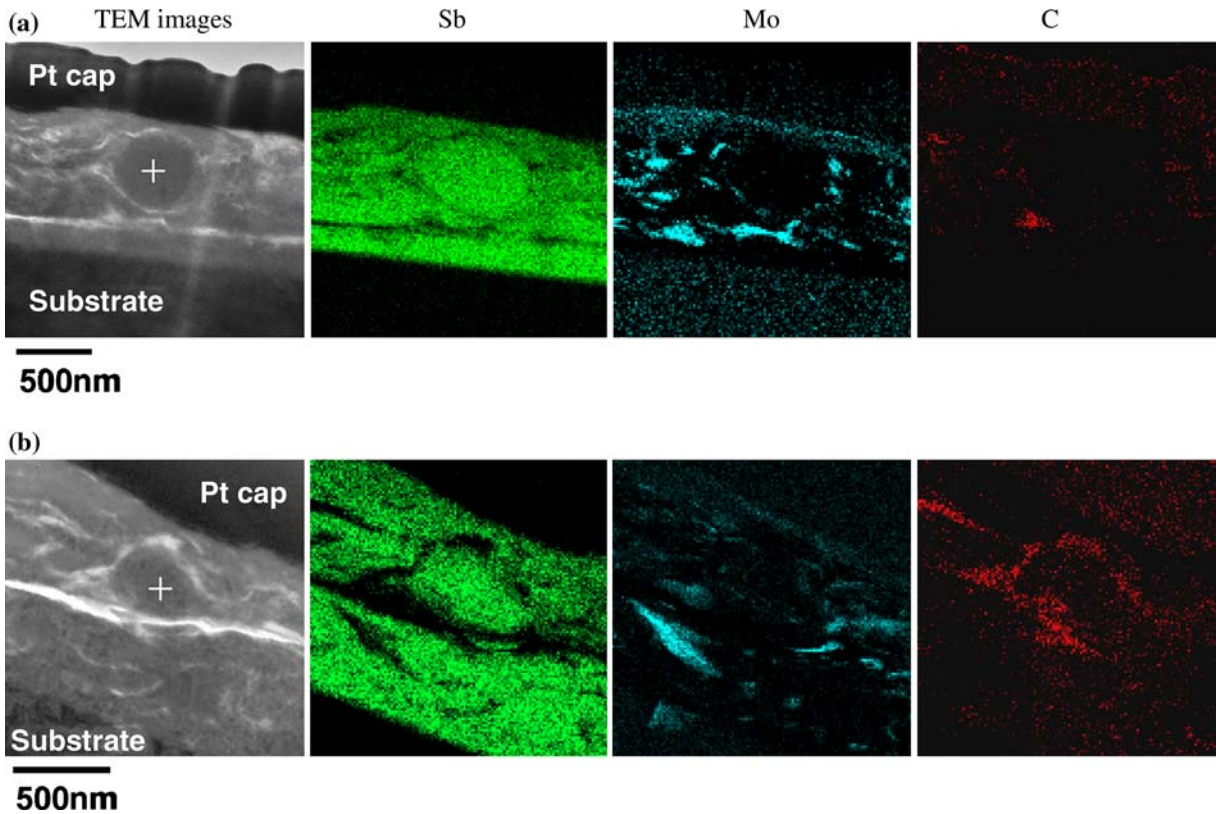

Figure 6. Nano probe energy dispersive spectrometer (EDS) elemental mapping of Sb, Mo and C for the cross-sectional specimen of wear scars: (a) in dry nitrogen, and (b) in humid air, where the corresponding cross-sectional TEM images are shown on left.

20 μm wide by 5 μm deep was cut with Ga^+ ion beams from inside the humid wear scar. First, the wear scars were studied across the whole film thickness between the Pt protection caps and substrates. Figure 6a, b show the nano-probe-EDS elemental mapping of Sb, Mo and C for the cross sections of dry and humid wear scars, respectively. The corresponding cross-sectional TEM images are given on the left, where the crosses indicate Sb_2O_3 particles just beneath the top lubricating layer in the film. Micro cracking was revealed inside the film, which developed along the direction of substrate surfaces. The distribution of Sb, Mo and C is shown in figure 6a, b. Of particular interest, MoS_2 surrounds the Sb_2O_3 particle inside the dry wear scar, as shown in figure 6a, while graphite surrounds the Sb_2O_3 particle inside the humid wear scar, as shown in figure 6b. A very thin layer of MoS_2 was visible in the EDS elemental mapping of Mo inside dry wear scar.

Figure 7a, b are the high-resolution TEM images taken from the above cross-sectional specimens for the top layers on dry and humid wear scars, respectively. The (002) basal planes of hexagonal MoS_2 were clearly visible on the dry wear scar, as shown in figure 7a, while the basal planes of graphite was measured on the humid wear scar, as shown in figure 7b. Those basal planes are approximately parallel to the sliding direction and are in the best orientation for hexagonal MoS_2 and graphite materials to provide lubrication [20,21]. The present TEM measurements further verified the effective lubrication of hexagonal MoS_2 in dry/vacuum tests and graphite in humid tests for the burnished MoS_2–Sb_2O_3–C composite films. TEM images demonstrate that the outer most (or exposed) interface is the active lubricant for the environment where the tribotest was run. The Raman data provided a better physical picture of the chemistry near the surface compared to AES.

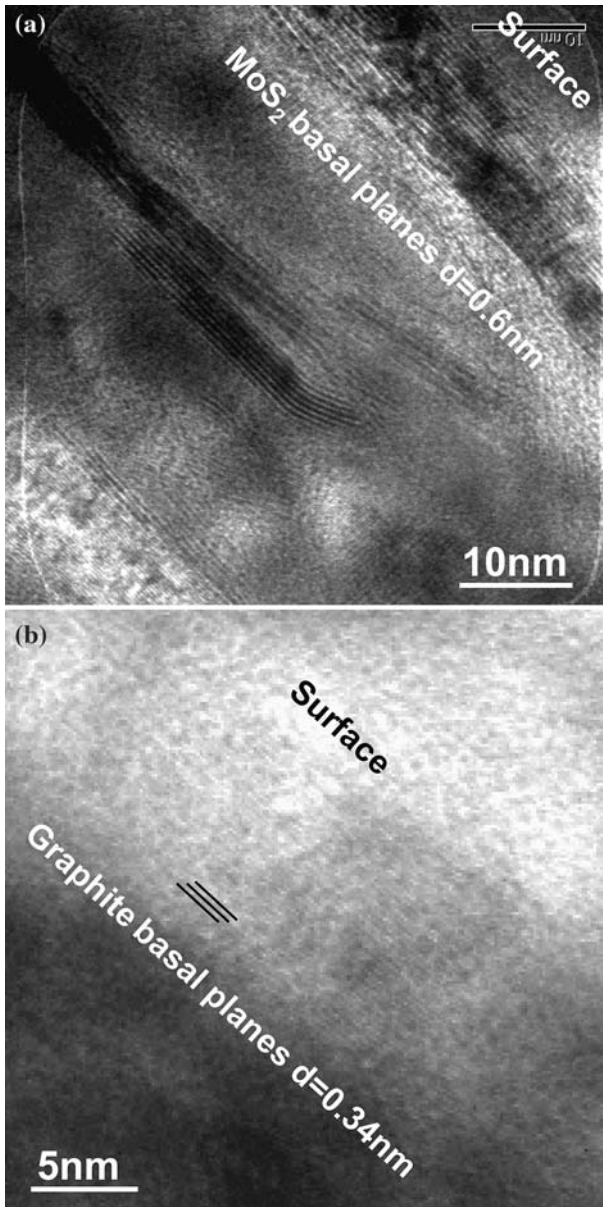

Figure 7. High-resolution TEM images taken from the cross-sectional specimen of wear scars: (a) in dry nitrogen, and (b) in humid air.

3.4. Tribological behavior in environmental cycling

Many tribological applications require stable performance in environments with varied humidity. Figure 8 shows an example of friction coefficient variation in a tribotest where the environment varied every 5000 sliding cycles between humid air (50% RH) and dry nitrogen for the burnished MoS_2–Sb_2O_3–C composite film. This test procedure can simulate friction in ambient/space cycling because friction and wear results for dry nitrogen and vacuum were similar, and humid air/high vacuum cycling was more difficult to implement. In humid cycles, the friction coefficients were about 0.15–0.25, and corresponded to lubrication by graphite. In dry cycles, the friction coefficients decreased to less than 0.05, corresponding to lubrication by MoS_2. A slightly higher friction was recorded for both humid and dry cycles, in comparison to the measurements under a constant humid/dry condition as shown in figure 1a, b. A few thousand cycles were not sufficient to develop a complete steady-state lubricious tribofilm on counterpart surfaces such as that formed after ten thousand cycles of humid or dry tribotests. In general, if cycling is stopped, the friction will approach the long-term single environment value.

To study the environmental adaptability and lubrication mechanism of burnished MoS_2–Sb_2O_3–C composite films, the above multi-cycling humid/dry tribotests were stopped in the middle of humid and dry cycles, respectively. The samples were analyzed using a micro-Raman spectroscope in order to determine the predominant phase at the rubbing contact. For the dry cycle, Raman activity was observed in the MoS_2 region and almost no carbon-related scattering was detected, as

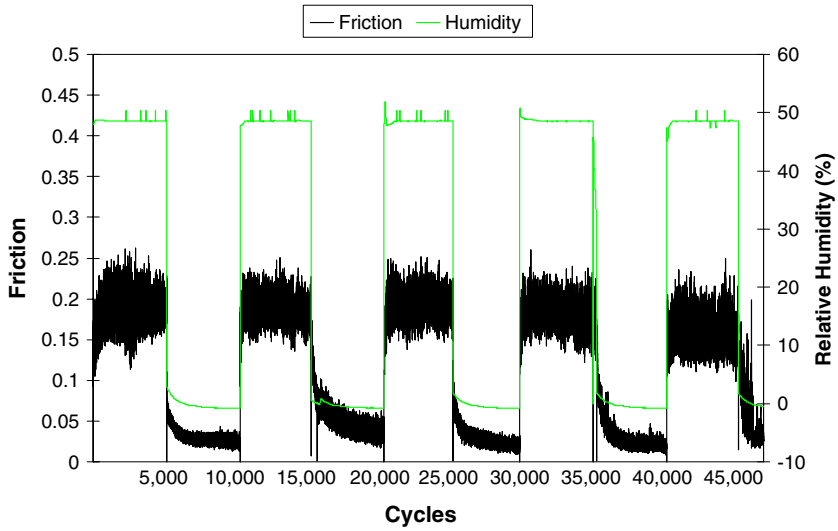

Figure 8. Friction coefficient variation in tests for the environment varied from humid air [50% relative humidity (RH)] to dry nitrogen every 5000 cycles.

shown in figure 9a. For the humid cycle, the signal from graphite-like carbon was clearly identified in the Raman spectrum, as shown in figure 9b.

Based on the measured friction variation and the analyses of wear scars, the following lubrication mechanism was proposed for the environmental adaptability of burnished MoS_2–Sb_2O_3–C composite films. In dry conditions, which are favorable for MoS_2, but severe for graphite, there is a predominant formation of hexagonal MoS_2 at the contacting interfaces. It is created by sliding/rubbing stress. These layers are oriented such that the basal planes are parallel to the surface. This densely packed (002) surface is the most oxidation resistant, inert, and slippery crystal face. Once the humidity is increased, the MoS_2 layers on counterfaces were replaced by basal oriented graphite where again the basal surface is most inert and slippery. For graphite, the intercalation of basal planes with water molecules is essential for low friction and wear rate [22,23]. In the next dry cycle, the desorption of water molecules results in rapid wear-off of graphite sheets, which reveals fresh MoS_2 grains and causes debris with MoS_2 to recoat the surface. The friction-induced reorientation of MoS_2 basal planes promotes low friction and low wear in dry tests, and so on. The orientation and density of the layer helps prevent deep oxidation.

In addition, Sb_2O_3 forms a sublayer for the active lubricant as discussed in earlier publications [9,14]. The cross-sectional TEM images in figure 6 show that the Sb_2O_3 particles are not simply coated on the surface by the active lubricant. The particles must roll and tumble till all surfaces of the particles are covered. Rubbing causes enrichment and orientation of the active lubricant at the surface of Sb_2O_3. This has a positive effect on lubrication because: (1) the best lubricant and crystal orientation are achieved at the interface; (2) thin layers of lubricant on a harder material provide lower friction; (3) a thin layer of lubricant on top of an oxide results in some containment of oxidation caused by a friction-driven thermal spike; and (4) the tumbling/rolling of Sb_2O_3 particles acts somewhat like a "pump"

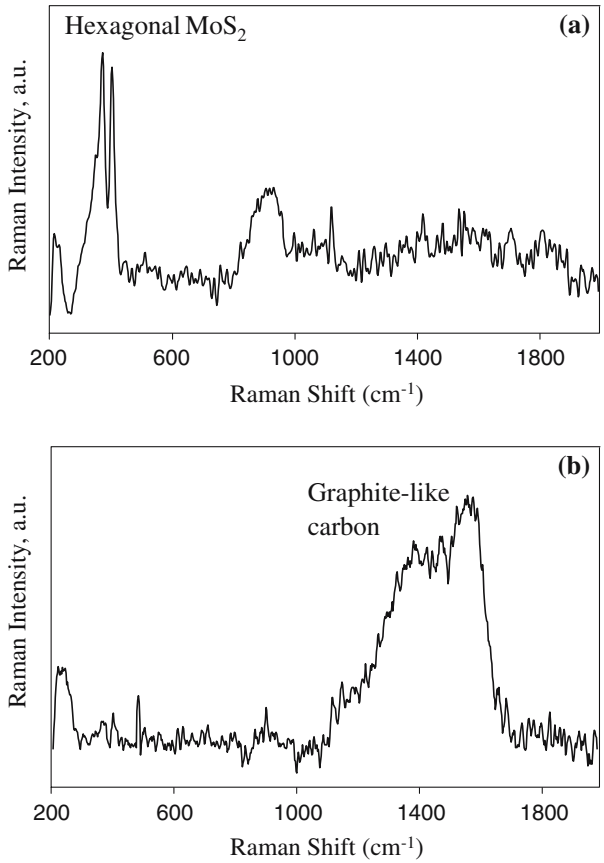

Figure 9. Raman spectra collected from the wear scars on the burnished MoS_2–Sb_2O_3–C composite film as the multi-environmental friction measurement was specially stopped: (a) at dry nitrogen cycles where strong MoS_2 signals are indicated, and (b) at humid air cycles where only graphite-like carbon signals are indicated.

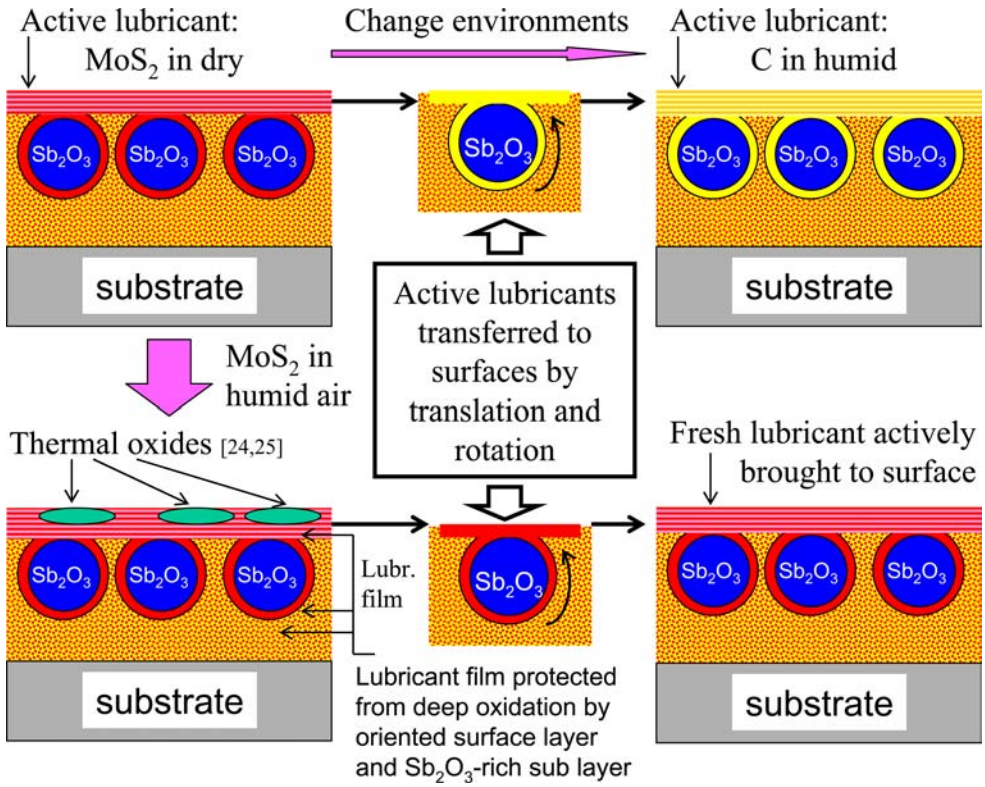

Figure 10. A series of schematic diagrams of the lubrication mechanism proposed for MoS_2–Sb_2O_3–C composite films.

to provide lubricant to the rubbing interface. Figure 10 shows a series of schematic diagrams of the above proposed lubrication mechanism for MoS_2–Sb_2O_3–C composite films. An active lubricant layer was generated over the surface of Sb_2O_3 particles. This self-layered microstructure and the composite nature of the film helps inhibit crack formation and growth, which is very important for increasing wear-life especially when changing atmosphere. It was noted earlier that cracking precedes failure. The Sb_2O_3 particles inside the film can effectively block the propagation of cracks perpendicular to the substrate and hence slow the film delamination/wear-off.

4. Conclusions

1. The MoS_2–Sb_2O_3–C composite film prepared by simply burnishing process showed lower friction and longer wear-life than the pure MoS_2 film and pure graphite film in humid air. Very/super low friction and nearly unlimited wear-life were measured in the environments of dry nitrogen and vacuum.
2. All characterization results by means of Raman, TEM and AES indicated that the hexagonal MoS_2 played superior lubrication in dry/vacuum tribotests and the graphite composition effectively lubricated in humid tribotests for the burnished MoS_2–Sb_2O_3–C composite films. The synergistic effect of graphite and Sb_2O_3 additives with MoS_2 improve tribological properties.
3. In dry conditions, a predominant formation of hexagonal MoS_2 is created by sliding/rubbing stress at the contacting interfaces. These layers are oriented such that the basal planes are parallel to the surface. This densely packed (002) surface is the most oxidation resistant, inert, and slippery crystal face. Once the humidity is increased, the MoS_2 layers on counterfaces were replaced by basal oriented graphite where again the basal surface is most inert and slippery.
4. The active lubricant layer of MoS_2 or graphite was generated over the surface of Sb_2O_3 particles. This self-layered microstructure and the composite nature helps inhibit crack formation and growth, which is very important for increasing wear-life especially when changing atmospheres. The Sb_2O_3 particles inside the film can effectively block the propagation of cracks perpendicular to the substrate and hence slow the film delamination/wear-off.
5. Burnished MoS_2–Sb_2O_3–C composite films are easily deposited, low-cost lubricant films, which were used to understand chameleon behavior and showed remarkably good performance, especially extremely low friction in dry and vacuum environments.

Acknowledgement

The Air Force Office of Scientific Research (AFOSR) is gratefully acknowledged for financial support.

References

[1] A.J. Haltner and C.S. Oliver, Nature 188 (1960) 308.
[2] S.F. Calhoun, F.S. Meade, G.P. Murphy and R.L. Young, Lubric. Eng. 21 (1965) 97.
[3] R.P. Pardee, ASLE Trans. 15 (1972) 130.
[4] M.T. Lavik, R.D. Hubbell and B.D. McConnell, Lubric. Eng. 31 (1975) 20.
[5] P.W. Centers, Tribol. Trans. 31/32 (1987) 149.
[6] P.W. Centers, Wear 122 (1988) 97.
[7] C.J. Klenke, Trib. Intl. 23 (1990) 23.
[8] J.S. Zabinski, M.S. Donley, V.J. Dyhouse and N.T. McDevitt, Thin Solid Films 214 (1992) 156.
[9] J.S. Zabinski, M.S. Donley and N.T. McDevitt, Wear 165 (1993) 103.
[10] B.C. Stupp, Thin Solid Films 84 (1981) 257.
[11] T. Spalvins, Thin Solid Films 118 (1984) 375.
[12] M.R. Hilton, R. Bauer, S.V. Didziulis, M.T. Dugger, J.M. Keem and J. Scholhamer, Surf. Coat. Technol. 53 (1992) 13.
[13] K.J. Wahl, L.E. Seitzman, R.N. Bolster and I.L. Singer, Surf. Coat. Technol. 73 (1995) 152.
[14] J.S. Zabinski, M.S. Donley, S.D. Walck, T.R. Schneider and N.T. McDevitt, Tribol. Trans. 38 (1995) 894.
[15] D.G. Teer, J. Hampshire, V. Fox and V. Bellido-Gonzalez, Surf. Coat. Technol. 94–95 (1997) 572.
[16] A.A. Voevodin and J.S. Zabinski, in: *Nanostructured Thin Films and Nanodispersion Strengthened Coatings*, A.A. Voevodin, D.V. Shtansky, E.A. Levashov and J.J. Moore, eds. (Kluwer Academic Publishers, Dordrecht, Netherlands, 2004), pp. 1–8.
[17] A.R. Lansdown, in: *Molybdenum Disulphide Lubrication*, D. Dowson, ed. (Elsevier, Amsterdam, 1999).
[18] F.G. Fisher, A.D. Cron, R.G. Muber, *NGLI Spokesman*, Vol. 46 (National Lubricating Grease Institute, 1982), p. 190.
[19] M.N. Gardos, Tribol. Trans. 31 (1988) 214.
[20] V. Buck, Wear 91 (1983) 281.
[21] J. Moser and F. Levy, Thin Solid Films 228 (1993) 257.
[22] R.H. Savage, J. Appl. Phys. 19 (1948) 1.
[23] M.N. Gardos, in: *Proceedings of 1st Tribology Congress on New Directions in Tribology*, London, 8–12 September 1997, Institute of Mechanical engineers, London (1997), Paper 229.
[24] P.D. Fleischauer, J.R. Lince, P.A. Bertrand and R. Bauer, Langmuir 5 (1989) 1009.
[25] P.D. Fleischauer and J.R. Lince, Tribol. Int. 32 (1999) 627.